1-1-2005

Friction and asperity contact in strip rolling

A. K. Tieu
University of Wollongong, ktieu@uow.edu.au

Zhengyi Jiang
University of Wollongong, jiang@uow.edu.au

Cheng Lu
University of Wollongong, chenglu@uow.edu.au

Prabuono B. Kosasih
University of Wollongong, buyung@uow.edu.au

Friction and Asperity Contact in Strip Rolling

Anh Kiet TIEU, Zhengyi JIANG, Cheng LU and Buyung KOSASIH
(School of Mechanical, Materials and Mechatronics Engineering, University of Wollongong, NSW 2522 Australia)

Abstract: This paper reviews different aspects of friction and asperity contacts in strip rolling. The mixed film lubrication model considers the effect of asperity flattening and the lubrication within the working zone. The oil concentration of the emulsion at entry and throughout the roll bite is considered together with the thermal effects of the contacts. The actual area of contact due to asperity deformation can be determined from a 3-wavelength FEM model. The deformation of a randomly generated surface of the hot strip with oxide scale can also be modeled by an FEM method. The friction variation in the roll bite can be determined by a sensor roll, and the average friction determined from the forward slip by the marking method or laser Doppler method. The friction models in FEM modeling are also discussed.
Keywords: friction, asperity contact, lubrication, emulsion, FEM

1 Introduction

Fluid lubricants are widely used in cold rolling to improve the surface quality of the metal products, to reduce the mill power consumption and the roll wear. The lubrication mechanism should be in the mixed film regime, where the film is not sufficiently thick to completely separate the rolling surfaces and as a result metal-to- metal contact occurs at the surface asperities. A roll gap model would be more accurate if correct friction model is considered, as strip gauge and shape can be improved. The friction coefficient is normally assumed constant at the strip/roll interface. However, previous research have confirmed that the friction varied in the roll bite (Lenard [1], Liu, Tieu et al. [2]), and it affected the rolling pressure and the accuracy of on-line control models. Thus it is important to consider proper friction variation in any mathematical model for rolling. To determine accurately the friction, the following aspects have to be considered:

(i) asperity contact which involves actual area of contact and thermal effects;
(ii) the amount of emulsion lubricant at entry and that inside the work zone;
(iii) friction variation in the roll bite.

2 Mixed film lubrication

2.1 Model

A mixed-film friction model illustrated in Fig.1 has recently been developed and applied in the strip rolling simulation. The film pressure was determined from the Reynolds equation. Wilson et al. [3, 4], Qiu & Tieu [5] developed an analytical model for strip rolling in this

regime. In their model, the surface roughness was approximated by longitudinal saw-tooth topography, with the relationship between the contact area, deformation pressure and the film pressure determined using an upper bound theory. Fig.2 to 4 show the calculation results for different dimensionless speeds. From Fig.2, the friction hill is reduced at higher rolling speed. The reduced contact area and increased hydrodynamic pressure significantly reduces the friction (see Fig.4), which results in a lower deformation pressure P as shown in Fig.2. The mixed film lubrication model provides important information on roll bite contacts such as asperity contact, lubricant pressure, film thickness and frictional shear stress.

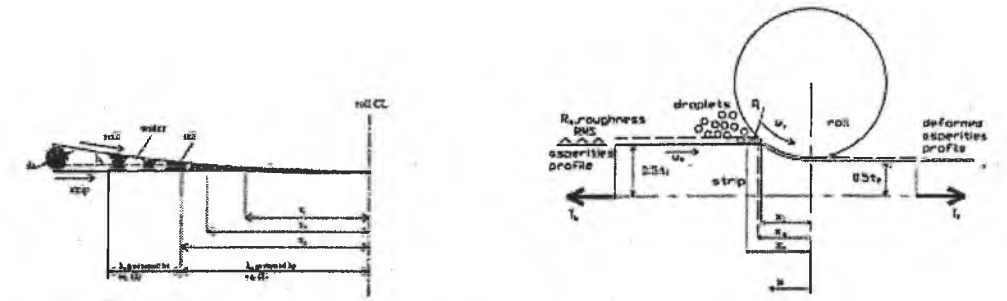

Fig. 1 Schematic of the rolling process

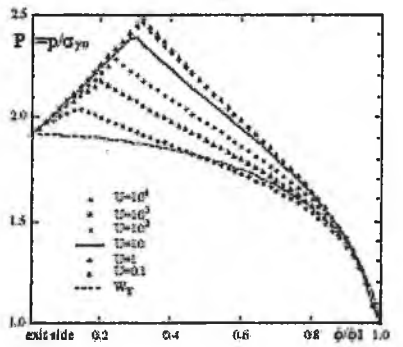

Fig. 2 Distribution of the deformation P

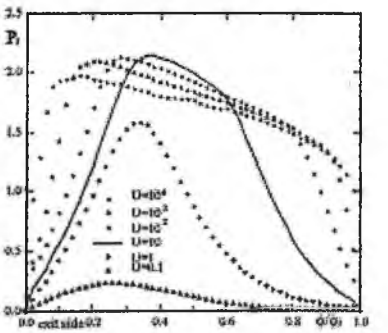

Fig. 3 Hydrodynamic film pressure P_f

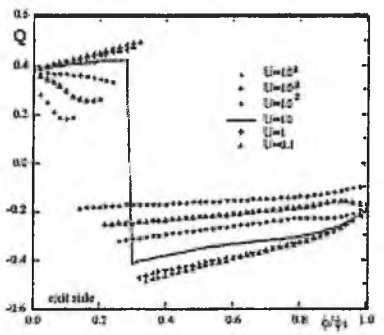

Fig. 4 Friction force along the roll bite

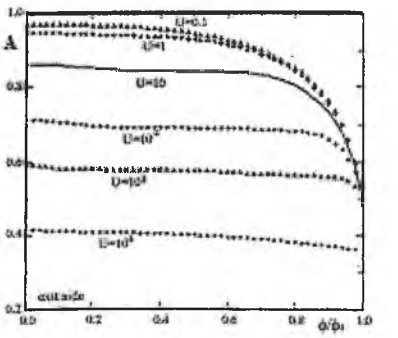

Fig. 5 Contact area in the roll bite

2.2 Thermal effects

Thermal effects in strip rolling operations play a significant part in a cold rolling production line, leading to problems such as high roll-strip interface temperature and non-uniform strip

temperature. The thermal field of a work roll dictates the thermal crown of the roll and affects strip shape. A comprehensive analysis of the thermal effects must take into account the following aspects: 1) heat generation due to plastic deformation of the strip and that due to frictional shear stress at the roll-strip interface; 2) heat conduction within the roll and the strip; 3) heat transfer across the roll-strip interface; and 4) heat transported by the rolled strip. Such an analysis must incorporate the mechanics of rolling, the hydrodynamics effect of the lubricant flow and the heat transfer in the roll and the strip. Tseng [6, 7], Wilson et al. [8] considered interface temperature of strip rolling. A feature introduced in the model is the partition coefficient which governs the fraction of frictional heat generated at the interface and transferred through the roll and the strip. The roll and strip temperature are shown in Fig.6.

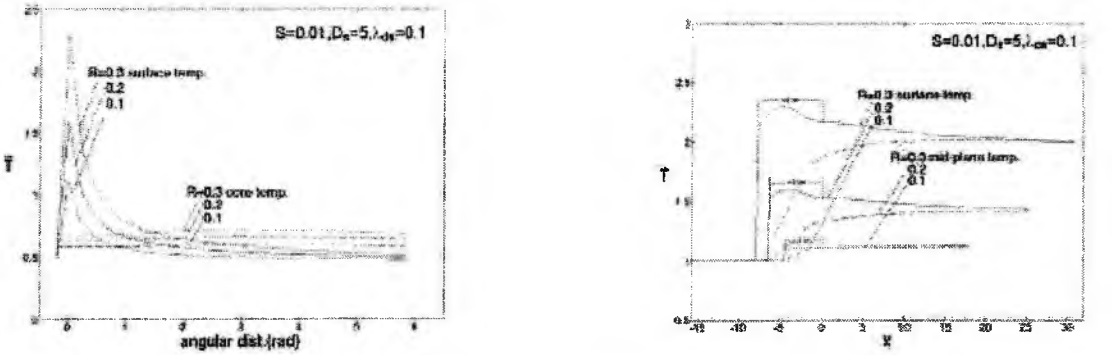

(a) roll (b) strip

Fig. 6 Roll surface and core temperature (a) and strip surface and mid-plane temperature (b) for different reduction R; S = 0.01, λd = 0.1, Ds = 5, Tb = Tf = 0

2.3 Rolling lubrication using O/W emulsions

The frictional condition at the roll-workpiece contact in the deformation region is largely controlled by the type of lubricant chosen for a particular application. Oil-in-water (O/W) emulsions have been widely used, and they generally contain 1% to 5% volume of oil with typical droplet diameter in the range from 2 to 20μm. Theories describing its lubrication mechanism in EHL line contact have been presented [9-11]. Tieu & Kosasih [12-14] found that significant oil concentration transforms the emulsion from being water-based to oil-based with water as the dispersed phase and enables the emulsion to provide oil-like lubrication in the contact zone (Fig.7). The mechanism of how droplets are captured is not well understood. Experiments [15] show that it is related to rolling speed, and droplet sizes and oil concentration of the emulsion. Computational fluid dynamics (CFD) and particle tracking techniques have been used to investigate the flow pattern and droplets motion in the inlet zone. Further analysis of a 2D flow suggests an existence of significant reverse flows (Fig. 8).

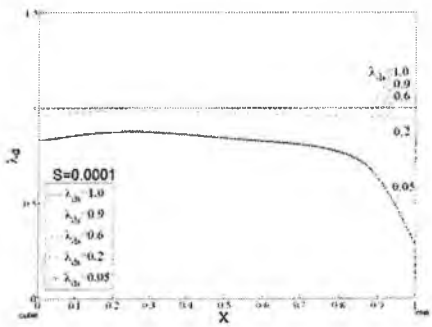

Fig.7 Concentration of the oil phase of the work zone

Fig. 8 2D streamlines showing reverse flows at the inlet ($U = 1.5\ ms^{-1}$).

3 Friction measurement

A number of cold rolling tests have been reported [16-19], all showing that the ratio of frictional stress to normal stress (friction coefficient) is indeed not constant along the contact length. The friction coefficient can be measured by either direct or indirect methods. Direct method refers to the sensor roll method which measures the friction variation point by point in the roll bite, and indirect method includes strip marking method and the Laser Doppler method [20], both of which determine the average friction coefficient from the measured forward slip. The friction can also be determined by an inverse method (see also section 4).

The direct measurement from sensors on the roll uses a set of pin-type transducers embedded in the work roll, as shown in Fig.9. The rolling pressure and interfacial shear stress in the roll bite could be obtained based on the force equilibrium of the radial and oblique pins. The friction coefficient in the rolling contact is determined from an analysis of the equilibrium of forces acting on the radial and oblique pins, as can be seen from an example of cold rolling in Fig. 10 and 11. Among hundreds of rolling tests in this laboratory, no multiple pressure peaks was found from the radial pins signals.

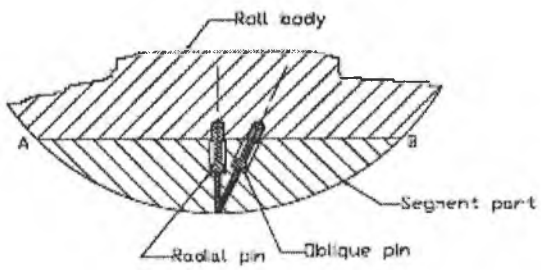

Fig. 9 Sensor roll section view

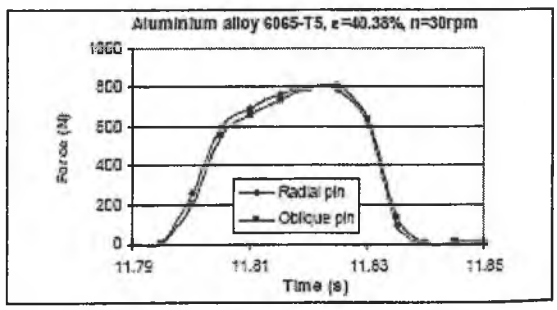

Fig. 10 Force distribution in cold rolling

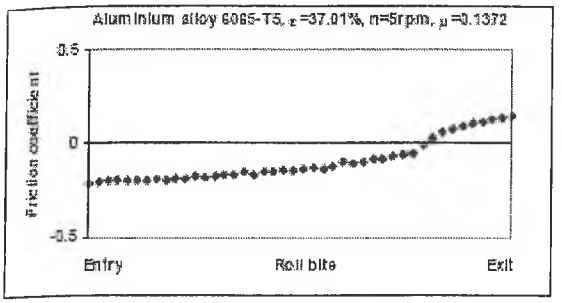

Fig. 11 Friction coefficient in cold rolling

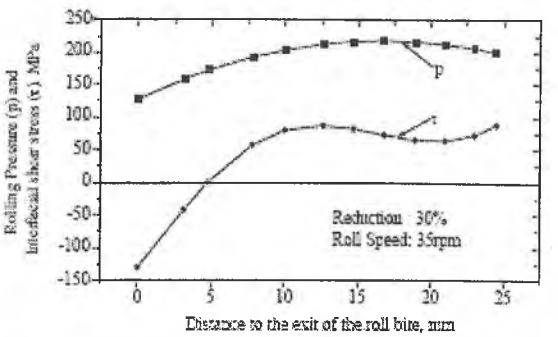

Fig. 12 Rolling pressure and shear stress (hot rolling)

The sensor roll was also used in the experimental hot rolling test. The rolling pressure and interfacial shear stress in the roll bite are shown in Fig.12. The interfacial shear stress shows the different trend in the forward slip area and backward slip area. In the strip marking method, the forward slip S_f is determined from a known circumferential length Lo between the known markers on the roll to imprint 2 markers of distance L' on the rolled strip [18]. The roll and strip exit speed u_r, u_{w2} can be measured by two Laser Doppler Velocimeter probes on the rolling mill [20] which determine the forward slip $s_f = (u_{w2} - u_r / u_r)$ and then friction. It has been found that the friction coefficient variation over the roll bite fits well with the fifth-order polynomial (Fig.13).

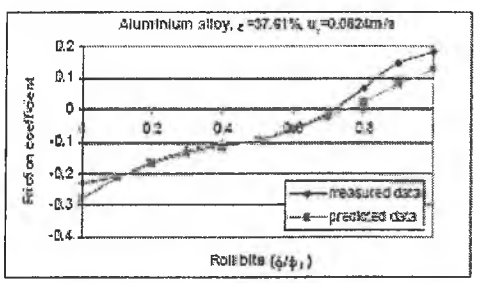

Fig. 13 Measured and predicted friction coefficient

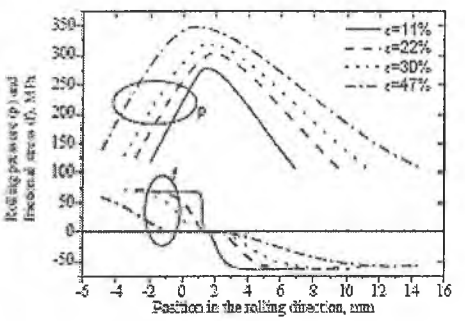

Fig. 14 Rolling pressure and shear stress

4 Friction variation by the inverse method

A multi-objective inverse method can also be used to determine the distribution of the frictional stress and coefficient of friction along the roll bite. In the inverse method, parameters (rolling force, rolling torque and forward slip) of the process are determined experimentally. A function with unknown parameters is assumed to represent the distribution of the frictional stress. The unknown parameters can be obtained by optimizing a combined target including multiple objectives, namely the measured rolling force, measured rolling torque and measured forward slip, under a yield condition at the roll bite exit. The results are shown in Fig.14 [21]

5 Asperity contact in cold rolling

5.1 Model

As one can see that when the asperities on strip surface are in contact with the roll, the valleys are filled with lubrication (Fig.15). Asperity flattening and lubrication behaviour together therefore control the friction activities at the interface and the strip surface finish. However, the contact mechanics of surface asperities under large plastic deformation is still a key issue when applying the model. The friction and the distribution of lubricant at the interfaces between the workpiece and tool are mainly affected by the actual area of contact and the surface roughness features [23-26].

Wilson and Sheu [23], Sutcliffe [24] Korzekwa et al. [27] have investigated the asperity flattening under bulk plastic deformation by an upper bound approach, a slip line field solution and a finite element model respectively. Kimura and Childs [25] discussed the effect of dimensional factors on the crushing of ridge-shaped asperities and variation of contact ratio under bulk plastic straining conditions. Sutcliffe [24] and Ma, Tieu et al [28] presented a two–scale wavelength and three-wavelength profile.

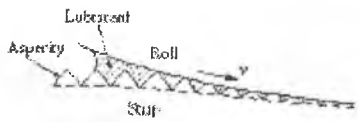

Fig. 15 Mixed-film lubrication in strip rolling

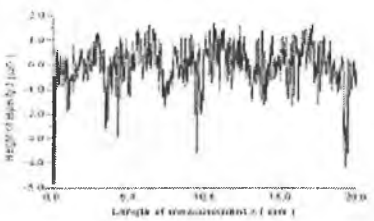

Fig. 16 A typical asperity profile of strip surface

The real contact area, evolution of surface roughness, distribution of friction force and contact pressure at the interface has been determined [28]. A random surface can be represented by a multitude of components of different wavelengths with a number of them having a dominant effect. The one-to three-wavelength profile of a typical steel strip surface (Fig.16) is shown in Fig.17 and an FEM asperity model in Fig.18.

5.2 Area of contact ratio

Fig.19 compares the evolution of area of contact ratio (A) with normal pressure obtained by the three FEM models for 1, 2 and 3 wavelengths, Keife's model[23] and Bay's experiment [26]. The area of contact ratio A, defined as the ratio of real to apparent area of contact, increases as a function of nominal pressure for all the three models. As more short-wavelength components are combined into the roughness model, there are more peaks appearing on the asperity surface. Fig.20 compares the ratio of roughness change (Ra′/Ra) obtained in simulation with experimental measurements [28], where Ra′ is the roughness after flattening while Ra is the initial roughness.

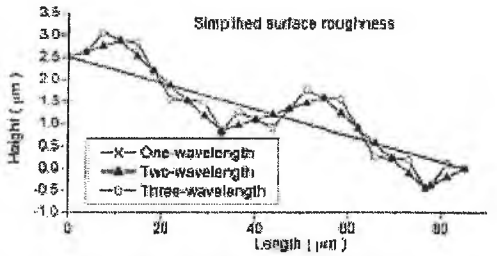

Fig. 17 Surface roughness simplification models

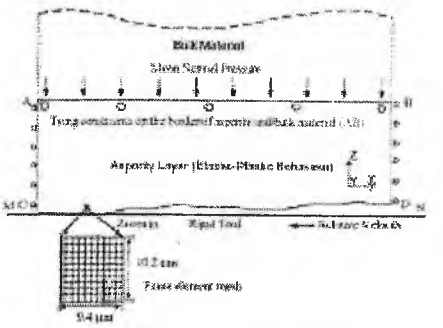

Fig. 18 FEM model setup (3-wavelength)

5.3 Friction force distribution at the interface

Fig.21 shows the evolution of friction force distribution along the contact surface with load steps under dry friction condition for the three-wavelength model. It is obvious, from Fig.21, that the contact friction forces are non-linearly distributed at the contact face for all the cases. As the normal pressure increases, the distribution of friction force becomes more non-uniform. Mabo, Tieu et al [28] found that friction force as well as the non-uniformity of its distribution at the interface increases.

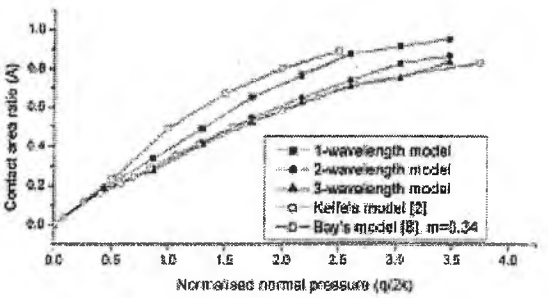

Fig. 19 Contact area

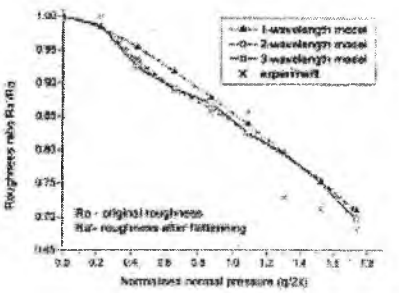

Fig. 20 Surface roughness

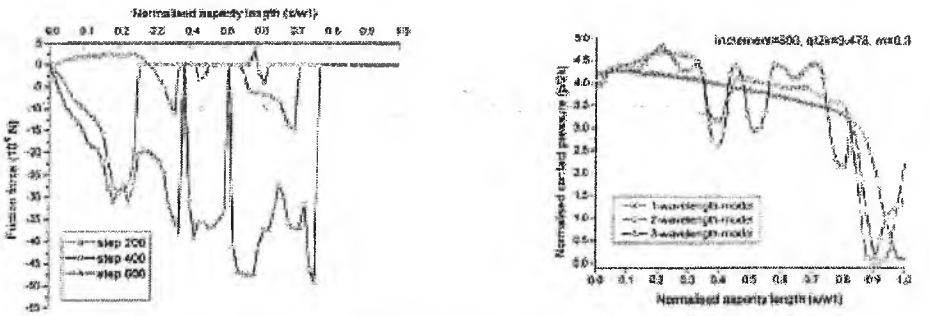

Fig. 21 Evolution of friction and contact pressure distribution along asperity surface of 1 to 3-wavelength model

5.4 Contact pressure distribution at the interface

Fig.21 shows the evolution of contact normal stress or contact pressure distribution along the asperity surface for 3-wavelength model respectively. The contact pressure clearly increases with the increment and distribution of contact pressure is not uniform for all cases. This kind

of distribution leads to a large pressure concentration and sharp variation on the entire asperity surface. It can produce a higher local temperature rise, influence the friction and lubrication at the tool/workpiece interface, and tool wear.

6 Theoretical determination of friction

6.1 Ploughing/adhesion friction model

In cold strip rolling the surfaces of the tool and metal are microscopically rough and consist of a multitude of apparently random peaks and valleys. The much harder tool's asperities are expected to plough into the surface of the softer workpiece. A ploughing/adhesion model has been developed by Lu and Tieu [29] to predict friction in cold strip rolling without any a-priori assumptions. The upper bound method is used to describe the ploughing phenomenon and molecular dynamic (MD) method is used to predict the local friction at the real contact area.

6.2 Ploughing model

The upper bound method is used to model the ploughing process. It is assumed that the stationary tool asperity has a rhombus-based pyramidal shape and the rigid-perfectly plastic workpiece moving at the velocity u_0 has a flat surface. The tool asperity ploughs the workpiece surface as shown in Fig.4. The workpiece flows by a rigid tetrahedron block (OABE) around each side of the asperity and forms a side ridge. Fig.23 shows the coefficient of friction (Ft/Fn) against the asperity angles in the transverse direction (α_1) and in the moving direction (α_2) respectively.

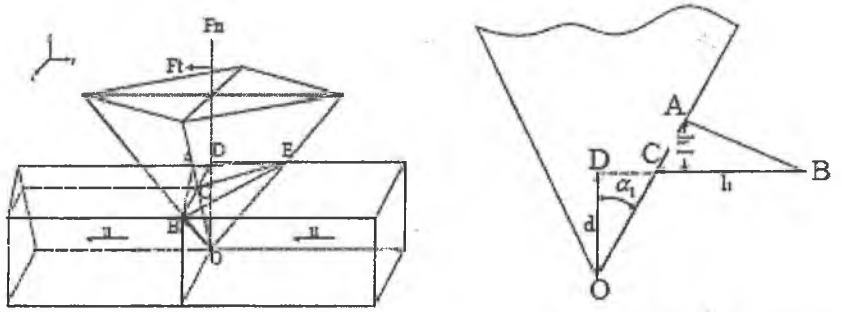

(a) General view (b) Left side view

Fig. 22 Schematic of the asperity ploughing process

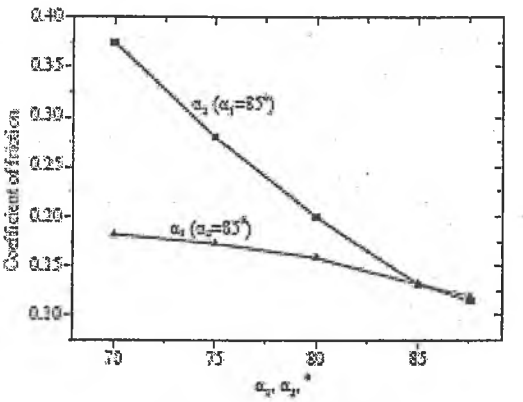

Fig. 23 Coefficient of friction

7 Contacts in hot rolling

Exposure of metals and alloys to high temperatures leads to the formation of oxide scales. To determine the composition of oxide scale layers and its deformation characteristics, oxidation tests [30, 31] were carried out at 800, 900 and 1000°C with 0.3-160s oxidation time. Fig.24 shows the thickness ratio of magnetite in the oxide layers of the mild steel when the oxidation was carried out at 900°C. Generally, the magnetite scale layer thickness increases with temperature. At the same time, the higher the oxidation temperature, the thicker the Fe_3O_4 layer will be (Fig. 24) [31]. A number of studies have concentrated on the contacts and oxide scale deformation in hot strip rolling [32-35].

It can be seen from Fig.25 [32] that friction reduces with entry temperature and rolling speed. The sample entry temperature reduces the friction coefficient for lubricated conditions (See Fig.25). The effect of oil-lubrication on reducing mill loads is rather significant, and more so at low temperatures.

An examination on the effect of emulsion lubricant on friction coefficient and mill loads on Fig. 27 indicates the effectiveness of oil-lubrication in reduction less than 35% [30, 31]. At a higher reduction, the 1:100 oil/water mixed emulsion proves to be more effective.

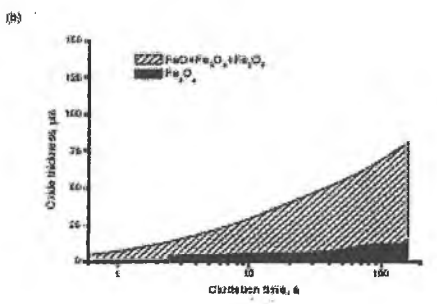

Fig. 24 Thickness of magnetite in the oxide layers of mild steel at 900°C

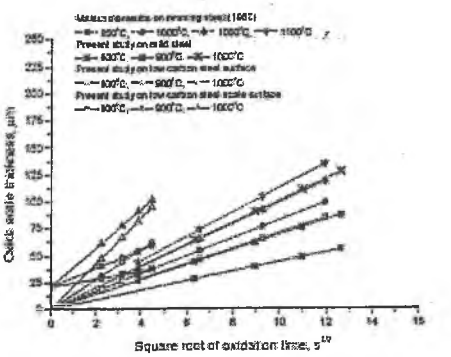

Fig. 25 Oxide scale thickness

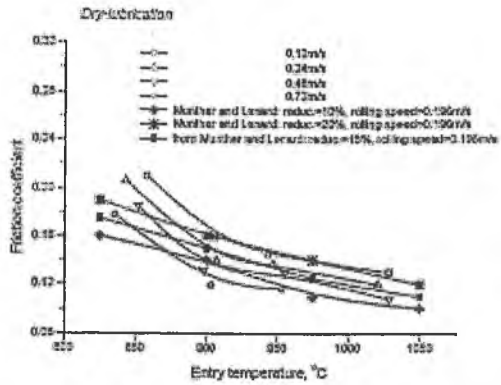

Fig. 26 Effect of entry temperature on friction coefficient at various rolling speeds under non-lubricated conditions, Reduction range: 23.4-16.3%

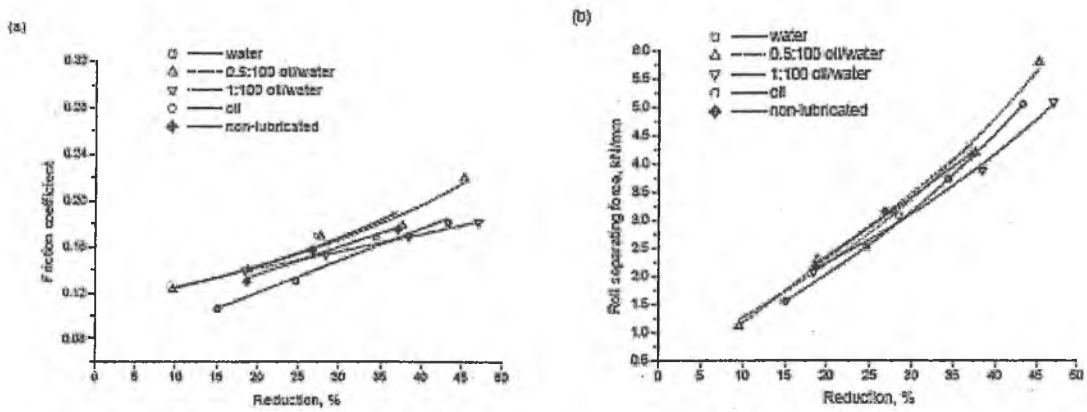

Fig. 27 Effect of lubricating conditions on friction coefficient and milling loads at various reductions: Rolling speed=0.11m/s and entry temperatures between 895-935°C;
(a) friction coefficient and (b) roll separating force

The friction coefficient for hot rolling as function of rolling parameters such as reduction, speed and temperature has been empirically derived[30, 31] .

$$u_{non-\text{lub}} = 0.405 + 0.0047\varepsilon - 0.057\upsilon - 0.00033T \quad (1)$$

$$u_{non-\text{lub}} = 0.138 + 0.0028\varepsilon - 0.017\upsilon - 8.17\times10^{-5}T \quad (2)$$

in which ε is reduction in "%", ν is the roll velocity in "m/s" and T is temperature in °C. The range for the three parameters is respectively 6.4-35%, 0.09-0.72m/s and 835-1030°C.

8.1 Model of Surface Profile for hot Rolling

In this model, the surface profile or surface section profile is formed by joining a series of profiles of single roughness asperities. Each profile of roughness asperity (or the shape of roughness asperity) can be described by the same function. For the 3-dimensional case, the profile of an asperity can be randomly generated as shown in Fig.28, Tang, Tieu et al [36, 37].

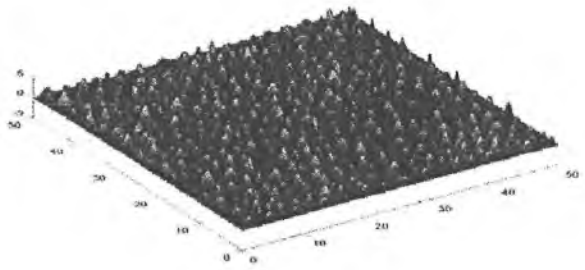

Fig. 28 3D surface profile generated from the model

8.2 FEM modeling of asperities

The thickness of scale varies for different rolling stage. After descaling, the scale is thin when the hot strip enters the finishing mill. Experiments indicate that the scale consists of three layers, FeO, Fe_3O_4 and Fe_2O_3, however a simplified two-layer model illustrated in Fig.29 can be used.

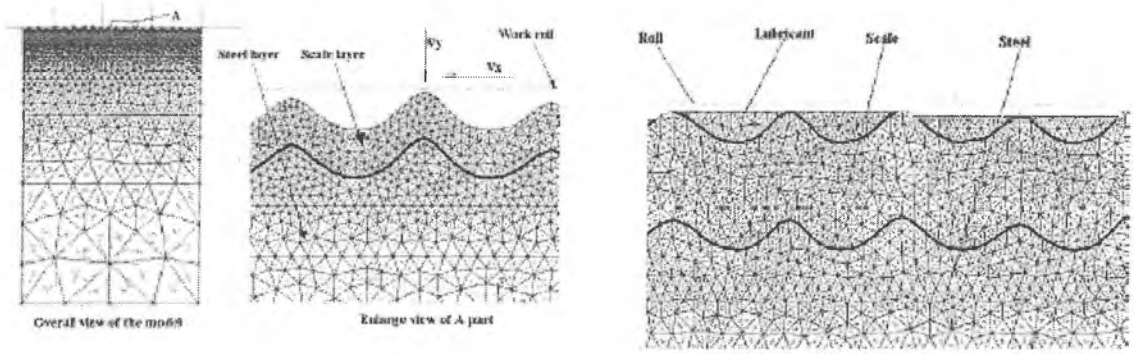

Fig. 29 Simplified FEM model for rolling process with scale layer with and without lubricant filling the valleys of the strip surface

8.3 Effect of lubrication

In hot strip rolling, when an emulsion lubricant is applied, the lubricant adheres to the work roll and is then in contact with the strip surface. The effect of the lubricant falling on to the strip surface on the roughness deformation can be divided into 2 types. In one case the lubricant is isolated inside the deformation zone, whereas in the other case the lubricant from different valleys is connected. The volume of the lubricant inside the roll bite is influenced by the pressure and the flow of the metal deformation. Inside the deformation zone, the strip scale may contact the work roll and the lubricant directly. The lubricant flows inside the deformation zone and exerts pressure on the strip surface. The scale and steel surface roughness are reduced slightly less when lubricant is connected inside the deformation zone (Fig.30).

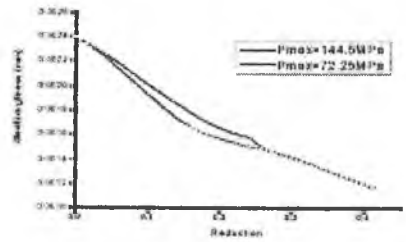

Fig. 30 Effect of lubricant pressure on steel surface roughness

8.4 Model of Scale Crack

In the simulation, it is assumed that scale only cracks in some positions where the tensile stress exceeds the strength of weakened location. Of course the crack opening may or may not allow the steel metal to protrude upward, and the strip surface roughness is modified accordingly. For a rolling reduction of 40%, initial scale roughness: 1 μm and scale thickness: 10.5 μm, the final crack width is 1.27μm for a cracking tensile force of 30 MPa and 0.92 μm for 100MPa.

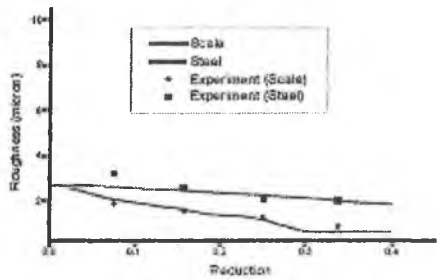

Fig. 31 Roughness versus reduction (lubricated)

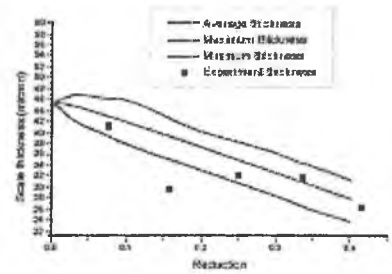

Fig. 32 Scale thickness versus reduction

9 Friction considerations in finite element modeling

The slightly compressible materials model has been employed to solve many kinds of rolling problems by the 3D rigid plastic FEM, Liu [38]. Jiang & Tieu [39-40] employed the rigid plastic FEM to solve the strip rolling taking into account the friction variation in the deformation zone. According to the variational principle, the real velocity field must minimise the following functional:

$$\phi - \iiint_v \bar{\sigma}\bar{\varepsilon}dv + \iint_{S_f} \tau_f \Delta V_f ds + \iint_{S_K} \tau_K \Delta V_K ds \pm \iint_{S_v} \tau_v ds$$
$$= \phi^p + \phi^f + \phi^j + \phi^t$$

where the second term on the right hand side is the work rate of friction (φ^f); ΔV_f is the relative slip velocity at the interface of the strip and the rolls where the frictional shear stress τ_f is applied. There are a number of frictional shear stress models that can be used. One is a constant friction model 1, $\tau_f = m_1\sigma_s/\sqrt{3}$ in the deformation zone, or friction variation model 2 proposed by (Kobayashi et al. [41]).When the sticking friction occurs in the vicinity of the neutral point, the friction zone can be modelled according to Kragelsky [42]. The distributions of these frictional shear stress models are shown in Fig.35 (k is the shear yield stress).

Results from the model in Fig.35a are shown in Fig.35 (k is the shear yield stress). Results from the model in Fig.35a are shown in Fig.36. The results of the simulation with mixed friction 1 (Fig.35b) is close to the measured values (calculated rolling pressure 96 MPa and forward slip 4.2% compared to measured values 96.04 MPa and 4.1%) [40].

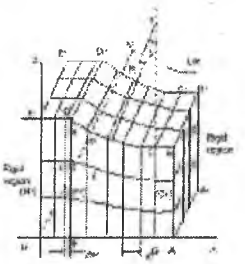

Fig. 33 3D-FEM model

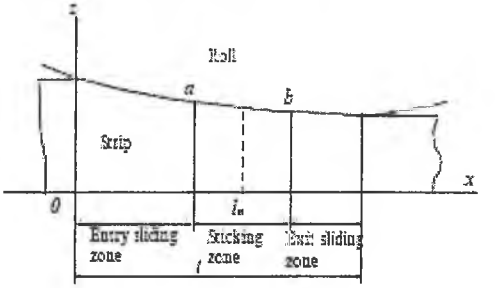

Fig. 34 Different regime of friction for hot rolling (Fig.35b)

10 Conclusions

This paper has highlighted the importance of a number of factors affecting the friction and asperities in the strip rolling process, namely:

- asperity flattening and the lubrication within the working zone.
- oil concentration of the emulsion at entry and throughout the roll bite.
- thermal effects of the contacts.
- friction variation in the roll bite (measured and calculated).
- scale morphology and its deformation in hot rolling.
- friction consideration in FEM modeling.

Any rolling model needs to take them into account to improve the quality of the end products.

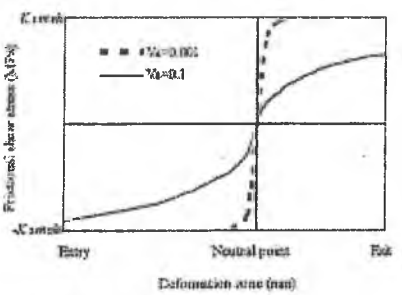

(a) Friction variation

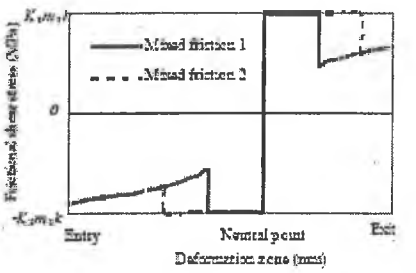

(b) mixed variation

Fig. 35 Frictional shear stress models

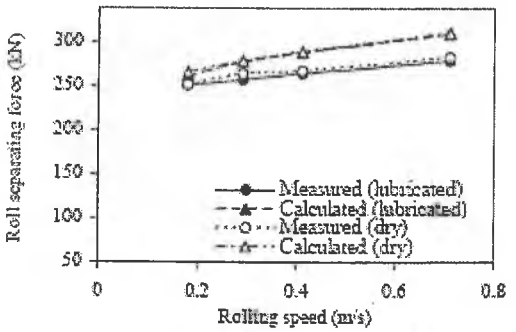

Fig. 36 Calculated rolling force and measured values (Model in Fig. 35a)

Acknowledgements

The authors acknowledge the support of an ARC Discovery grant. We are grateful to Mr. W. Sun and Mr. J. Tang for their contribution.

References

[1] J.G. Lenard, Friction and forward slip in cold strip rolling, Tribology Trans., 1992, 35: 423.

[2] Y.J. Liu, A.K. Tieu, E,B, Li and W.Y.D. Yuen, Forward slip and friction in cold rolling, Proceedings of International Symposium on Advanced Forming and Die Manufacturing Technology (AFDM'99), Pusan, Korea, September 7-9, 1999: 495-500.

[3] Wilson, W.R.D. & Chang, D.F. Low speed mixed lubrication of bulk metal forming processes. Tribology in manufacturing processes, ASME publication, CRTD-Vol 30, Trib-Vol 5, PED. 1994, 69: 159-167.

[4] Chang, D.F. & Wilson, W.R.D., Lubrication of strip rolling in the low-speed mixed regime. Tribology transactions, 1996, 39(2): 407-415.

[5] Qiu,Z.L, Yuen,W.Y.D., & Tieu, A.K. The mixed-film lubrication theory and tension effects on metal rolling process. ASME J. Tribology. 1999.

[6] A.A. Tseng, Thermal modeling of roll and strip interface in rolling processes: part 1 - review, Numerical Heat Transfer Part A, 1999, 35: 115-133.

[7] Tseng, A.A., Thermal characteristics of roll and strip interface in modeling rolling processes, Journal of Materials Processing & Manufacturing Sciences, 1997, 6: 3-17.

[8] Wilson, W.R.D., Chang, C.T., Sa, Y.T., Interface temperatures in cold rolling, Journal of Materials Shaping Technology, 1989, 6: 229-240.

[9] Wilson, W.R.D., Sakaguchi, Y., Schmid, S.R., A dynamic concentration model for lubrication with oil-in-water emulsions, Wear, 1993, 161: 207-212.

[10] Kimura, Y., Okada, K., Lubricating properties of Oil-in-Water Emulsions, Tribology Transactions 1989, 32: 524-532.

[11] Yan, S., Kuroda, S., Lubrication with Emulsion: First Report, The Extended Reynolds Equation, Wear, 1997, 206: 230-237.

[12] P.B. Kosasih, A.K. Tieu, W.H. Li, C. Lu (2005), The effects of oil concentration and droplet diameter in oil-in-water emulsion on strip rolling, Proceedings of International Conference on Technology of Plasticity, Oct. , Verona, Italy.

[13] A.K. Tieu, P.B. Kosasih, (2005) Computational Fluid Dynamics Analysis of Oil Droplet Captures Mechanism in Strip Rolling, 32nd Leeds-Lyon Symp. on Tribology, Sept. 2005, Lyon, France.

[14] A.K. Tieu, P.B. Kosasih, (2005) Thermal Effect on Mixed Film Lubrication Strip Rolling with O/W Emulsion Lubricant, 32nd Leeds-Lyon Symposium on Tribology, Sept. 2005, Lyon, France.

[15] Nakahara, T., Makino, T., Kyogoku, K., Observations of liquid droplet behavior and oil film formation in O/W type emulsion lubrication, Trans. ASME, J. of Tribology, 1988, 110: 348.

[16] G.T.V. Rooyen and W.A. Backofen, Friction in cold rolling, Journal of the Iron and Steel Institute, 1957, 186: 235-244.

[17] A. Banerji and W.B. Rice, Experimental determination of normal pressure and friction stress in the rolling gap during cold rolling, Annals of the CIRP, 1972, 21: 53-54.

[18] F.A.R. Al-Salehi, T.C. Firbank and P.R. Lancaster, An experimental determination of the roll pressure distribution in cold rolling, Intl Journal of Mechanical Sciences, 1973, 15: 693.

[19] Y.J. Liu, A.K. Tieu, D.D. Wang and W.Y.D. Yuen, Friction measurement in cold rolling, Journal of Materials Processing Technology, 2001, 111: 142-145.

[20] A.K. Tieu, E.B. Li and W.Y.D. Yuen, Forward slip measurements in cold rolling using Laser Doppler Velocimetry, Proceedings of 7th International Conference on Steel Rolling,1998, Chiba, Japan, The Iron and Steel Institute of Japan, 145-149.

[21] C. Lu, A. K. Tieu, P. B. Kosasih, H. B. Ren and Z. Y. Jiang, (2005) Finite Element Simulation of 3D Surface Asperity Flattening in Metal Forming, International Conference on Advanced Manufacture, Nov. 2005, Taipei, Taiwan.

[22] Wilson, W.R.D. and Sheu, S. "Real area of contact and boundary friction in metal forming", Int. J. Mech. Sci., 1988, 30(7): 475-489.

[23] Keife, H. and Sjögren, C. "A friction model applied in the cold rolling of aluminum strips", Wear, 1994, 179: 137-142.

[24] Sutcliffe, M.P.F. "Flattening of random rough surfaces in metal-forming processes", J. Tribology, 1999, 121: 433-440.

[25] Kimura, Y. and Childs, T.H.C. "Surface asperity deformation under bulk plastic straining conditions", Int. J. Mech. Sci., 1999, 41: 283-307.

[26] Bay, N. and Wanheim, T. "Real area of contact and friction stress at high pressure sliding contact", Wear, 1976, 38: 201-209.

[27] Korzekwa, D.A., Dawson, P.R. and Wilson, W.R.D. "Surface asperity deformation during sheet forming", Int. J. Mech. Sci., 1992, 34(7): 521-539.

[28] Ma, B., Tieu, A.K. , Lu, C. and Jiang, Z. " A finite-element simulation of asperity flattening in metal forming", J. Mat. Proc. Tech., 2002, 131-132: 450-455.

[29] C. Lu, A.K.Tieu, Development of a ploughing/adhesion friction model and its application in cold strip rolling, Proc. Leeds-Lyon Symposium on Tribology, Lyon France 2005.

[30] Sun, W.H., Tieu, A.K., Jiang,Z. and H.T. Zhu, Effect of hot rolling conditions on deformation behavior of oxide scale at high temperatures, Key Engineering Materials, 2004, 274-276: 511.

[31] Sun, W.H., Tieu, A.K., Jiang,Z. and H.T. Zhu, (2004) Effect of Rolling Condition on mill load and oxide scale deformation in hot rolling of low carbon steel, Steel GRIPS Journal of Steel and Related Materials, 2002, 4: 579-583.

[32] P A. Munther, John G. Lenard, J. of Mater. Proces. Technology, 1999, 88: 105-113.

[33] F. Matsuno, Blistering and hydraulic removal of scale films of rimmed steel at high temperature, Trans. ISIJ, 1980, 20: 413-421.

[34] M. Krzyanowski, J. H. Beynon, The tensile failure of mild steel oxide under hot rolling conditions, Steel Res., 1999, 70: 22-27.

[35] J. H. Beynon, Y. H. Li, M. Krzyzanowski and C. M. Sellars, Metal Forming 2000: 331.

[36] Tang, J., Tieu, A.K. Jiang,Z, (2004) A simulation of surface roughness in hot strip rolling. In S. Ghosh, J.M. Castro, J.K. Lee (eds), Materials Processing and Design : Modelling, Simulation and Applications (NUMIFORM 2004): 630-635.

[37] J. Tang, A. K. Tieu and Z. Jiang Modelling of oxide scale crack in hot strip rolling, 8th Intl Conf. Tech. of Plasticity, Oct. 2005, Verona, Italy.

[38] Liu,X.H. Rigid Plastic FEM and its application in Steel Rolling, Beijing, Metallurgy Industrial Press, 1994.

[39] Tieu, A.K., Jiang, Z. Y., Lu, C. A 3-D finite element analysis of the hot rolling of strip with lubrication, Journal of Materials Processing Technology, 2002, 125-126: 638-644.

[40] Z. Y. Jiang, A. K. Tieu, C. Lu & W. H. Sun, (2002) Simulation of friction variation in hot strip rolling by 3D rigid plastic FEM, Proc. 3rd Australasian Congress on Applied Mechanics, Sydney 2002.

[41] Kobayashi, S., Oh, S. I. & Altan, T. Metal Forming and the Finite-Element Method. New York: Oxford University Press, 1989.

[42] Kragelsky, I. V. Friction and Wear Calculation Methods. Oxford: Pergamon Press, 1982.